JACS
JOURNAL OF THE AMERICAN CHEMICAL SOCIETY

ARTICLE

pubs.acs.org/JACS

Metadynamics Study of a β-Hairpin Stability in Mixed Solvents

Giorgio Saladino,[†] Stefano Pieraccini,[†,∥] Stefano Rendine,[†] Teresa Recca,[‡] Pierangelo Francescato,[‡] Giovanna Speranza,[‡] and Maurizio Sironi*[,†,§,∥]

[†]Dipartimento di Chimica Fisica ed Elettrochimica, Universita' degli Studi di Milano, Via Golgi19, 20133 Milano, Italy,
[‡]Dipartimento di Chimica Organica e Industriale, Universita' degli Studidi Milano, via Venezian 21, 20133 Milano, Italy
[§]CNR-ISTM, Istituto CNR di Science eTecnologie Molecolari and [∥]INSTM UdR, Via Golgi 19, 20133 Milano, Italy

Supporting Information

ABSTRACT: Understanding the molecular mechanisms that allow some organisms to survive in extremely harsh conditions is an important achievement that might disclose a wide range of applications and that is constantly drawing the attention of many research fields. The high adaptability of these living creatures is related to the presence in their tissues of a high concentration of osmoprotectants, small organic, highly soluble molecules. Despite osmoprotectants having been known for a long time, a full disclosure of the machinery behind their activity is still lacking. Here we describe a computational approach that, taking advantage of the recently developed metadynamics technique, allows one to fully describe the free energy surface of a small β-hairpin peptide and how it is affected by an osmoprotectant, glycine betaine (GB) and for comparison by urea, a common denaturant. Simulations led to relevant thermodynamic information, including how the free energy difference of denaturation is affected by the two cosolvents; unlike urea, GB caused a considerable increase of the folded basin stability, which transposes into a higher melting temperature. NMR experiments confirmed the picture derived from the theoretical study. Further molecular dynamics simulations of selected conformations allowed investigation into deeper detail the role of GB in folded state protection. Simulations of the protein in GB solutions clearly showed an excess of osmoprotectant in the solvent bulk, rather than in the protein domain, confirming the exclusion from the protein surface, but also highlighted interesting features on its interactions, opening to new scenarios besides the classic "indirect mechanism" hypothesis.

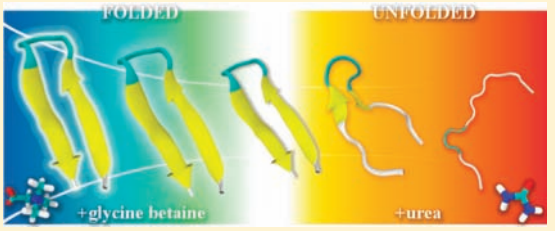

INTRODUCTION

Extreme environments, such as those found in deserts, deep abyssal waters, and icy lands, are characterized by severe adverse conditions, involving extreme temperatures, pressures, or salinity levels. Nonetheless, these regions are far from inhabitable; indeed, evolution has granted some mechanisms that allow the survival of living species, named extremophiles, in such harsh conditions. Several barophilic bacteria, as Psychromonas hadalis, for example, proliferate optimally at pressures of 50 MPa,[1−3] while Methanopyrus kandleri, a hyperthermophilic organism, can grow at temperatures as high as 120 °C.[4,5] Unveiling the molecular mechanisms responsible for this uncommon adaptability is of primary importance especially under an agricultural perspective; drought tolerance, for example, as shown by some angiosperms, the notorious resurrection plants,[6,7] could be a relevant factor in overcoming the difficulties that still afflict crop production in many countries. Accumulation of small, highly soluble, molecules, called osmolytes, is generally connected with extremophilic behaviors.[8,9] Besides being simple everyday compounds, these molecules have no charge at physiological pH and are nontoxic even in high concentration, thus being "compatible solutes", harmless to cell machinery. One of the most notable and studied effect of osmolyte is their protection of protein native structures against denaturation by thermal or chemical agents. Regardless of the large ensemble of known proteins, only a few osmolyte molecules, as a result of an accurate evolutionary selection, are able to protect them through a mechanism that de facto must be extremely general. This is a mechanism that despite multiple efforts is still to be unraveled. Two different hypotheses have been formulated so far for both protecting and denaturing osmolytes, involving a "direct mechanism" or an "indirect mechanism". Different driving forces are proposed in the context of the two main strands, supported by different experimental or computational evidences that, nevertheless, are still a matter of debate.[10,11] The proposed indirect mechanism explains protecting or denaturing effects in terms of an overall change in water structure, generally endorsing a kosmotropic/chaotropic description of the co-solutes.[10,12−14] Urea and denaturing agents weaken water structure allowing for a better solvation of hydrophobic groups, while protecting osmolytes strenghtens water hydrogen bond network. On the contrary, direct mechanism involves generally a direct interaction of the osmolyte with the protein backbone or with amino acidic side-chains.[15−19]

Received: June 9, 2010
Published: February 14, 2011

dx.doi.org/10.1021/ja105030m | J. Am. Chem. Soc. 2011, 133, 2897–2903

Unfortunately, there is still little agreement over which contribution, backbone,[16,20] or side chain[21,22] should be the most relevant one. In this field, the most interesting results have been obtained by Bolen and co-workers who, using transfer free energy studies, proposed the so-called "osmophobic effect".[23] According to this theory, a "direct-but-unfavorable" interaction of protecting osmolytes with the protein backbone, resulting in an exclusion of the osmolytes from the protein surface, is proposed as the driving force for the protecting effect, since the native state is characterized by a less solvent exposed backbone, compared to the unfolded state. Unfortunately, so far the mechanism of action of both protecting and denaturing osmolytes is still a matter of debate, and an accurate and universal description of the behavior of these molecules is still needed.

Molecular modeling had proved to be a suitable tool for the investigation at an atomic level of the properties of osmolytes,[10,24−27] accessing informations that are difficult to obtain experimentally. Recently, Daggett et al.[12] were able to describe with molecular dynamics (MD) mixtures of urea and trimethylamine N-oxide (TMAO), confirming that TMAO counteracts urea denaturating effect, allowing a fine-tuning of the mixture properties and hence a higher adaptability to different conditions. Since osmolytes influence protein stability, a proper description of folding, albeit challenging, is a crucial requirement. Protein folding indeed can easily fall outside the time scale accessible to standard MD simulations.

We perform our simulations on a model hairpin peptide, the 16 residues C-terminal fragment of G protein B1 domain.[28] The ability of this peptide, which forms a β-hairpin in the intact GB1 protein, to form a secondary structure element even when isolated in solution[29] makes it an ideal model for the study of folding and secondary structure formation to the extent that it is among the most widely studied peptides[30,31] with experimentally determined kinetic and thermodynamic properties. For this reason, the folding mechanism of the GB1 β-hairpin, a fairly simple structure composed of two strands connected with a turn, is still investigated and the study of the effects of osmolytes molecules on its stability gives the opportunity, not only to better understand the protecting role of these molecules, but also to have a wider picture of the behavior of this highly studied protein fragment. Several computational studies have addressed the problem of β-hairpin folding mechanism by means of long MD simulations,[32] Monte Carlo techniques,[33] bias potential approaches,[34] replica exchange molecular dynamics,[35,36] and recently metadynamics.[37,38] Here we describe a comprehensive approach to the study of osmolytes that, combining computational methods that allow to accelerate conformational transitions, as metadynamics[39] and solute tempering metadynamics (STMetaD)[40] with conventional MD, is able to reproduce all the main features of the protecting effect. We performed simulations of the GB1 hairpin in solutions of glycine betaine (GB), a well-known osmolyte, and the results were compared with the behavior in water and in solutions of urea, a common denaturant. The effects of GB and urea on the β-hairpin stability were investigated evaluating free energy differences and melting temperature variations and analyzing at a molecular level the different observed conformations. This approach allowed one to obtain relevant thermodynamic informations and to carefully analyze osmolyte's molecules behavior on a microscopic scale, gaining interesting insights into their interactions. A careful experimental validation by NMR experiments confirmed computational results. While many studies have been performed for various proteins in urea solutions,[10,12,18,27,41] this is the first study to our knowledge reporting enhanced sampling simulations and free energy landscapes for a protein in protecting osmolytes solutions.

RESULTS AND DISCUSSION

Simulations were performed on three systems: β-hairpin in water, in 1 M solution of GB, and in 1 M solution of urea. Since the attention is focused on GB-protecting effects at a temperature close to the calculated melting one,[35] metadynamics were carried out at 350 K. The simulations allowed one to obtain the free energy surface (FES) as a function of the chosen collective variables (CVs) (Supporting Information Figure S1) from the history-dependent bias introduced by metadynamics. To evaluate the effects of the two cosolvents on the β-hairpin stability, the ΔG of denaturation was calculated, following Bussi et al.,[37] as

$$\Delta G_{F\rightarrow U} = k_B T \log\left(\frac{\int_F ds \exp\left(-\frac{G(s)}{k_B T}\right)}{\int_U ds \exp\left(-\frac{G(s)}{k_B T}\right)}\right)$$

where F and U denote, respectively, the regions corresponding to the folded and the unfolded basins. A value of 2.19 kJ/mol was calculated for the control simulation, meaning that the process is disfavored in water and the folded structure is the most stable. The ΔG for the simulation with GB was 9.78 kJ/mol, a considerable increase in respect to the control simulation, reproducing the osmolyte stabilizing effect. On the other hand, the simulation in urea reported a negative ΔG of −18.5 kJ/mol, in agreement with the denaturing effect of urea.

Considering that the eventual neglect of relevant degrees of freedom can lead to biased results in metadynamics runs, the coupling with replica exchange algorithms has been advised.[37] STMetaD was chosen, since it allows the use of a considerably lower number of replicas and a higher ΔT. The FES obtained at 350 K with the corresponding minima structures are reported in Figure 1 (FES for the first four temperatures are reported in Supporting Information Figure S2).

The new FES confirmed the results of previous simulations: the ΔG for denaturation resulted increased upon addition of GB and decreased upon addition of urea. The STMetaD in 1 M GB reported a ΔG of 13.78 kJ/mol at 350 K, a slight increase in comparison with the value reported by metadynamics. Also the simulation in 1 M urea revealed little variation, showing a ΔG of −16.42 kJ/mol. The ΔG for the control simulation resulted consistent with the previously obtained one with a slightly lower value of −5.24 kJ/mol. By and large, the results could be considered in good agreement. The morphology of the FES, moreover, showed considerable analogies with the corresponding metadynamics surfaces. The simulation in water showed two almost isoergonic basins for native and denatured structures with typical partially folded and misfolded conformations prevailing in the unfolded ensemble, in agreement with recent results by Parrinello et al.[38] The unfolded basin corresponded to very low values of both CVs (as the typical molten globule); completely destructured, high gyration radius, conformations reported a significantly higher energy. An estimate of the activation energy, assuming a two state mechanism, was calculated to be 11.3 kJ/mol. In the GB solution, the native minimum was considerably more stable and embraced a larger part of the CV space, reflecting a more flexible structure. The unfolded basin, corresponding to a

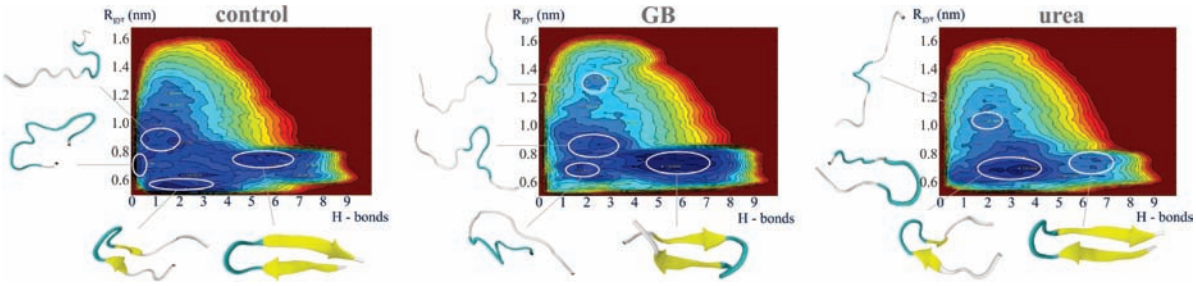

Figure 1. Free energy surface for STMetaD at 350 K (contours are spaced at intervals of 7 k_BT, energies are in kJ/mol). The most relevant minima are highlighted with the respective structures. The different conformations clearly showed that compact structures prevailed also in the unfolded ensemble with open destructured conformation having a rather high energy.

higher number of hydrogen bonds in respect to water-denatured structures, indicated a higher level of residual structure. Noticeably, a concomitant increase of the activation energy is observed, with an estimated value around 19.9 kJ/mol. The 1 M urea solution, on the other hand, presented a considerable increase of the native state energy and a prominent unfolded minimum that once more lies in a low gyration radius area of the CV space. Interestingly, no energy barrier for the evolution of the native structure into the denatured state was observed. In the approximation of a two state folding mechanism, the melting temperature T_m of the β-hairpin was calculated by linear regression of the ΔG values against the temperature.

The calculated T_m for the control simulation is found to be 340 ($\pm$6) K, apparently much higher than the reported experimental values of 297 K.[29] However, previous studies[35,42] have reported that a systematical overestimation of the melting temperature, highly dependent on the force-field parameters, is common to all computational results, giving values ranging from 330 to 485 K. Considering the ensemble of computational results, our estimation could be considered consistent with previously reported data, besides being in agreement with previous results[43] obtained with the same force field. Calculation of the T_m for the GB solution reported a value of 384 ($\pm$8) K, more than 40 K higher than the corresponding one in water. The urea solution, instead, reported a T_m of 329 ($\pm$3) K, confirming the opposite behavior of the two cosolvents. The moderate ΔT decrease strongly agrees with urea being generally used as a chemical denaturing agent in much higher concentrations to obtain complete unfolding at room temperature.

The trend of the thermodynamic data obtained from the simulations was confirmed by NMR analyses in aqueous solutions. We recorded NMR spectra in water at 278 and 288 K to observe the change of signals due to denaturation when passing from the low to the high temperature. From the 1H NMR spectrum recorded at 278 K (pH 6.3), we estimated the population of β-hairpin conformation to be ca. 49%. This was achieved referring to the sum of the absolute values of its C_α protons conformational shifts[44] to the same sum shown by residues 41−56 when assumed to be in 100% β-hairpin conformation.[29] At the higher temperature (288 K), the NOESY spectrum reported fewer and considerably weakened NOEs. In particular, the long-range NOE contacts involving the C_α hydrogens of Trp_{43} and Val_{54}, Tyr_{45} and Phe_{52}, and the side-chains of the aromatic residues, characteristic of the β-hairpin conformation, were no longer observable. On the other hand, NOE contacts between the amide protons ($d_{NN}(i, i+1)$) in the turn region (residues 46−51) remained unaltered, confirming previous results reporting a high stability of the turn region[30] and in agreement with the unfolded structures obtained from the simulations (see Figure 1). The β-hairpin content, as measured by the quantification method described above, was found to be ca. 39%. In agreement with the computational results, addition of GB in the ratio 1:10 at 288 K when the peptide in water was prevalently unfolded caused the equilibrium to be shifted toward the folded β-hairpin conformation with an estimated population of ca. 47%. On the other hand, addition of urea at 278 K when the β-hairpin is prevalently folded caused a considerable loss of NOE contacts, reporting a folded population of only 32%. These experimental results highlighted that a 1 M solution of urea, a concentration lower than the ones generally used for experimental denaturation assays, is nevertheless able to unfold this relatively small protein fragment, in agreement with the calculated ΔG.

Considering the nonequilibrium nature of metadynamics simulations, analyses at an atomic level of cosolvents configurations were performed on a set of standard "equilibrium" MDs. Folded structures representative of the native basin were extracted from the trajectory for every simulation. Preferential coefficients and solvent density functions (SDF) were calculated to investigate the cosolvents arrangement around the protein. Since a well-defined solvent bulk domain is needed for these evaluations, the selected system conformations were resolvated to obtain a larger 75 Å box to describe more properly the solvent properties at a relevant distance from the protein and to guarantee that bulk properties were constant and did not depend on the distance from the protein. During resolvation, additional water molecules were replaced with GB or urea to obtain a slightly higher concentration (2 M). Since the ratio between water and osmolytes molecules is crucial for the calculations, higher concentration simulations resulted being more suitable for statistical reasons, reporting more stable bulk averages. The calculated SDF for the mixed solvent simulations are reported in Supporting Information Figure S3). The cosolvent distribution around the protein revealed to be extremely different for GB and urea. The distribution in urea shows a prominent peak with a maximum corresponding to a well-defined distance value (1.8 Å). On the other hand, the curve for the GB solution shows to be below unity in the short-distance region (under 2 Å) where urea is accumulated and exceeds unity slightly only in the 2−4 Å region with a significantly broad peak, not showing a preferential interaction distance. The preferential coefficient Γ_{XP} confirmed the results of SDF analyses; for the 1 M GB simulation, the calculated value is negative (−1.28) meaning that, in the whole, GB is excluded from the protein surface, while urea simulations reported high positive values (6.84), consistent with an accumulation. In-depth analyses of the cosolvent distributions revealed a further difference between the two considered solutions (Figure 2) and largely explained the SDF trend.

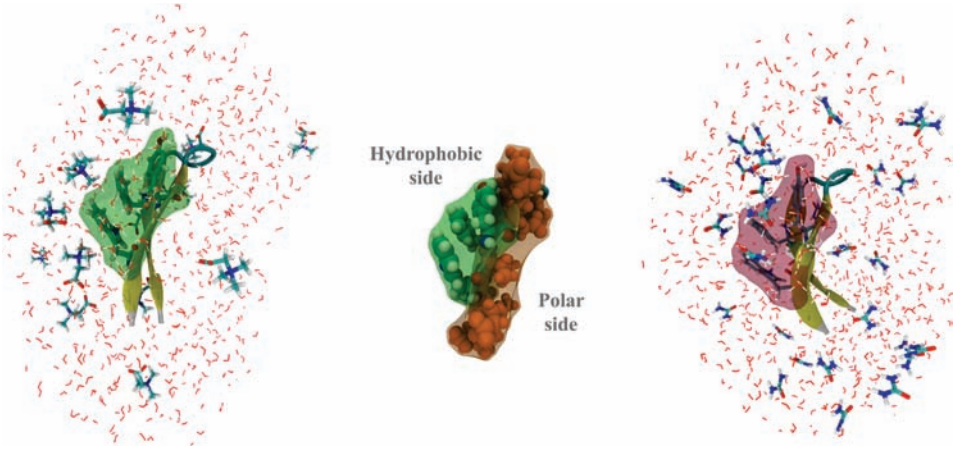

Figure 2. Preferential distribution of GB (left) and urea (right) around the hydrophobic core. The different polarity of the two sides of the hairpin is highlighted in the central panel. GB showed significant anisotropy in the distribution, being excluded by the majority of the residues, but interacting strongly with hydrophobic groups forming the core.

While urea distributed in a homogeneous way around the protein, GB had a marked anisotropic distribution, making contacts with the hydrophobic core, consisting of residues Trp_{43}, Tyr_{45}, and Phe_{52}. The hairpin, indeed, presented two distinct sides (see Figure 2, central panel): a hydrophobic side, where the side-chains of residues Trp_{43}, Tyr_{45}, and Phe_{52} clustered, and a more hydrophilic side with charged residues side-chains. GB prevalently accumulated on the first side, orientating the three methyl group toward the cluster and the carboxyl group toward the solvent. The preponderance of GB contacts with hydrophobic residues Trp_{43}, Tyr_{45}, and Phe_{52} is highly interesting because of their relevant role in β-hairpin stabilization.[45] The formation of the hydrophobic core involving these residues (Supporting Information Figure S4) has been described as the driving force for folded structure formation and is the fulcrum of many theories about hairpins folding mechanisms, based on the so-called hydrophobic-collapse.[31,33,36,46] Moreover, these residues are the ones reporting the most negative values of experimental transfer free energy according to Bolen et al.,[47] that is, the transfer of these residues from pure water to the osmolyte solution is highly favorable. These features are confirmed by calculation of the per residue preferential coefficient, Γ_{XP}^{RES} (Figure 3).

While on the whole, Γ_{XP}^{RES} trend confirmed the exclusion of GB from the protein surface, large positive values were obtained for Trp_{43}, Tyr_{45}, and Phe_{52}, confirming that the osmoprotectant was not excluded from these residues as opposed to the rest of the peptide and explaining the slight SDF increase compared to the bulk value in the 2−4 Å region. This minimal increase, indeed, is highly consistent with hydrophobic interactions between GB and the three listed residues considering the entity of the increase itself and the absence of a typical interaction distance. Interestingly, a marked apolar character of the solvent accessible surface area (SASA) is a constant for most of the osmolytes, as extensively discussed in a recent paper by Street et al.,[48] suggesting a significant importance of hydrophobic interactions and a possible screening of unfavorably solvated hydrophobic regions of the SASA by the protecting osmolytes that may contribute to the overall protecting effect. Urea, on the other hand, despite reporting the highest Γ_{XP}^{RES} for hydrophobic residues as GB simulations, clearly showed higher values also for the rest of the peptide, suggesting a direct interaction with the protein. For both urea and GB, the lowest values were reported for charged residues that, as expected, always preferred interactions with water molecules. Interestingly, the trend of urea Γ_{XP}^{RES} was in excellent agreement with previous results by Stumpe et al.;[17] preferential interactions were strong for hydrophobic residues, as Trp_{43} and Phe_{52}, and progressively weakened passing from neutral residues to polar ones and charged ones with negatively charged residues interactions being the most disfavored.

Predominant interactions with the protein backbone, as inferred in previous papers[17−19] were investigated calculating the backbone contribution to the preferential coefficient (Supporting Information Figure S5). Backbone contributions supported previous considerations, showing once more the exclusion of GB from the protein surface with the exception of hydrophobic residues. Backbone Γ_{XP}^{RES} for urea with only one exception reported always positive values even for charged residues, suggesting a strong interaction between urea and the peptidic main-chain. Once more, results for urea strongly agreed with previously reported ones,[18] proposing that urea acts as a "backbone surrogate". In-depth analyses of the contacts between protein and co-solvent (Supporting Information Figure S6) within a shell of 4.5 Å confirmed once more what was observed for the co-solvent distribution. Compared to water molecules, co-solvents seemed to spend most of the time around hydrophobic residues; the majority of the contacts with the protein for both urea and GB involved $_{43}$, $_{45}$, and $_{52}$ (Supporting Information Figure S7).

A further validation of the computational results and of the importance of the observed interaction was achieved through an accurate analyses of the NOE contacts and through their comparison with average distances calculated from the MD trajectories (Supporting Information Table T1). The observed NOE signals (Supporting Information Figure S8) were ranked on the basis of the average proton distance as weak (W, ca. 3.7−5.0 Å), medium (M, ca. 2.6−3.7 Å), or strong (S, ca. 2.2−2.6 Å). The comparison revealed a strong agreement between computational and experimental results. For GB, the NOE pattern was fully traced out by the distances calculated from the simulation of the folded state used for previous analyses. Most weak NOEs reported distances around 4−5 Å, while the medium and strong signals corresponded to lower proton−proton distances. For what concerned urea results, NOE distances were compared to a simulation of the unfolded state of the β-hairpin in 1 M urea,

dx.doi.org/10.1021/ja105030m |*J. Am. Chem. Soc.* 2011, 133, 2897–2903

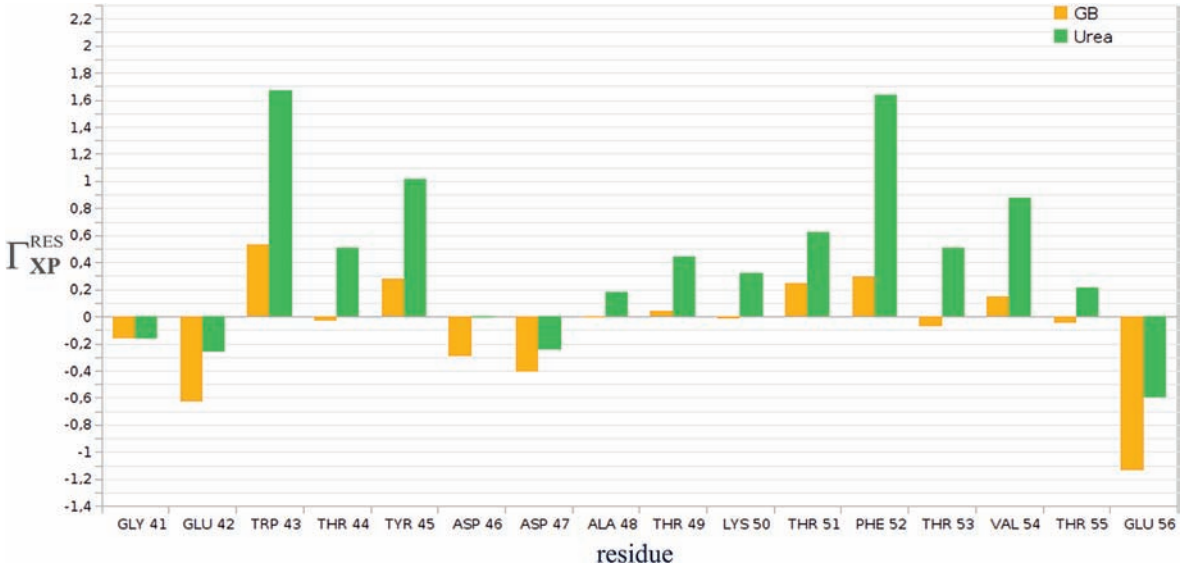

Figure 3. Preferential coefficient per residue. Values are generally positive for urea and negative or close to zero for GB. On the whole, hydrophobic residues are the ones with the highest Γ_{XP}, while charged residues always preferred interactions with water molecules. It can be inferred that the osmoprotectant is not excluded from hydrophobic residues (as Trp_{43} and Phe_{52}) as opposed to the rest of the peptide.

obtained using the same protocol used for folded states simulations. Again, the NOE trend was found to be in strong agreement with MD predictions since all side-chains contacts, whose NOE signal disappeared, reported a distance of more than 8 Å.

CONCLUSIONS

A proper description of the few experimentally observed features of osmolytes behavior is a mandatory starting point for a detailed and atomistic study of their mechanism of action. Mainly based on transfer free energies,[45,47] many models had been developed aimed at this purpose of pursuing a universal molecular theory. In the present study, we performed metadynamics, STMetaD, standard MD simulations, and NMR experiments of a model β-hairpin in GB solutions and in water and urea solutions, for comparison. Although the use of enhanced sampling techniques for the study of folding is more and more common, simulations of proteins in protecting osmolytes solutions had been carried out so far only by means of conventional MDs. Since the effect of cosolvents is deeply connected with protein denaturation, we combined the approach generally used to study protein folding with the computational tools developed to analyze osmoprotection mechanisms. This approach was able to fully describe osmolytes effects without "a priori" assumptions and to reproduce completely all the known behaviors of both GB and urea, including osmoprotectants exclusion from the protein surface, previously observed scatteredly with different computational and experimental techniques. Moreover, our results allowed to gain new interesting insights into osmolytes behavior and mechanism of action. The prevailing exclusion of GB from the protein surface, confirmed by Γ_{XP} calculations, strongly suggests that the protecting effect, largely reproduced by our simulations, must be ascribed to an indirect effect on the bulk solvent, consistent with the indirect mechanism hypothesis[13] reported in literature. However, no significant variation to water structure was observed in our simulations, possibly due to the low concentration. Our results, hence, while not excluding a "structure-making" effect on water, are more consistent with the indirect mechanism formulation proposed by Patey,[14] according to which the major protecting effect is connected with a dehydration of the protein first solvation shell and a decrease of the water molecules available for denaturation due to strong osmolyte−water interactions. For urea, a "direct mechanism" is strongly supported by our results where dispersion interactions play the dominant role, as previously reported in literature.[49,50] In addition, our simulations also provided evidence of hydrophobic interactions between the osmolyte GB and some protein residues, previously strongly put forward by direct mechanism promoters[21,22] and connected to a possible "screen effect" of the unfavorably solvated hydrophobic SASA regions. To our knowledge, this is the first atomic level observation of such interactions for GB alongside osmolytes exclusion from the protein surface. Considering the limited number of residues involved in these interactions, however, it is unlikely that their contribution would be the leading one. On the contrary, a "two-fold mechanism" hypothesis could be formulated, according to which the main contribution to the protecting effect is due to the solvent, while secondary effects, highly dependent on the nature of the protein SASA, can arise from direct interactions between the osmolytes and hydrophobic residues.

MATERIALS AND METHODS

The model protein chosen for the simulations is the β-hairpin fragment of G protein, obtained from G protein PDB structure (PDB code: 2GB1).[28] Three different systems had been set up: protein in water (control), protein in 1 M GB, and protein in 1 M urea. Metadynamics simulations were performed using GROMETA 2.0,[40] a modified version of GROMACS 3.3.3,[51] with OPLSAA force field.[52] The systems were solvated with TIP3P water molecules[53] in a cubic box with a side of 50.0 Å. A sufficient number of waters were replaced with GB or urea molecules to reach the correct concentration in all simulations except the control one. Three minimizations were performed with a steepest descent algorithm minimizing respectively the protein alone, the mixed solvent, and finally the entire system. Two different 50 000 step equilibrations were performed, the first being NVT, and the second being NPT. NPT conditions were then applied for all the production phase, using a temperature of 350 K and Nosé−Hoover thermostat.[54]

dx.doi.org/10.1021/ja105030m |*J. Am. Chem. Soc.* 2011, 133, 2897–2903

Integration step was 2 fs. Particle Mesh Ewald method[55] was used for long-range electrostatic interactions along with a 0.8 nm cutoff. The CVs were chosen accordingly to a previous work by Parrinello et al.[37] as the most suitable for the discrimination of folded and unfolded structures. Hence, the number of hydrogen bonds in the peptide backbone is calculated as

$$N_H = \sum_{i\in H}\sum_{j\in O}\frac{1-(r_{ij}/d_0)^6}{1-(r_{ij}/d_0)^{12}}$$

with $d_0 = 2.3$ Å, taking into account only the most relevant ones, that is, those with an odd, larger than four, sequence separation.[37] The radius of gyration is calculated as

$$R_{\mathrm{gyr}} = \sqrt{\sum_i \left(r_i - \frac{1}{N_a}\sum_j r_j\right)^2}$$

with summations running over all the N_a heavy atoms. The height of the gaussians is 1.0 kJ/mol, while the width is 0.1 along hydrogen bonds number and 0.01 along gyration radius. Gaussians are deposited every 100 steps. Each metadynamics run was scheduled for 25 ns but were considered concluded upon convergence of the free energy difference between the folded and unfolded state for more than 5 ns. Solute tempering metadynamics were performed on the same systems using 10 temperatures in geometrical progression in the range 300−507 K. This time, the height w of the gaussians for the replica m was rescaled with the corresponding temperature T_m, according to $w_m = 1.0k_BT_m$. Swapping between neighboring replica was attempted every 0.2 ps. The average acceptance rate for the Monte Carlo-like configuration swap, verified a posteriori, fell in the ideal range between 30 and 40%. All other parameters were maintained unaltered with respect to the first metadynamics runs. MD simulations of the most favorable folded/unfolded conformations were performed with the same parameters of the metadynamics runs. To better sample the bulk properties, at a relevant distance from the protein for preferential coefficient evaluation the protein has been resolvated in a larger box of 75 Å. All the MD runs were carried out for 11 ns.

Preferential coefficients (Γ_{XP}) were calculated using the approach proposed by Baynes and Trout[56−58] on the basis of previous works.[59,60] According to this theory, Γ_{XP} can be evaluated defining two domains, a bulk domain (I) and a protein one (II), and calculating

$$\Gamma_{XP} = \left\langle n_X^{II} - n_W^{II}\left(\frac{n_X^{I}}{n_W^{I}}\right)\right\rangle$$

where $n_{W/X}$ are the number of water (W) or osmolyte (X) molecules in the I/II domain. The molecules were subdivided into the different domains comparing their distance from the protein van der Walls surface with the chosen cutoff (4.5 Å). The calculation allows the computation of the solvent density function (SDF)[56] that describes how the molecule of osmolyte are distributed around the protein. In principle, it is equivalent to the radial distribution function but takes into account the shape and volume of the protein. The SDF is computed as

$$\rho_X(r) = \frac{X(r,r')}{V(r,r')}$$

where r is the radius of the solvation shell, $X(r,r')$ is the number of X molecules found from r to r', and $V(r,r')$ is the volume of the shell from r to r'. The number of molecules was obtained calculating for different bulk/protein separations, that is, different r values. The volume $V(r,r')$ was calculated on the basis of the grid-based solvent-accessible methodology by Daggett et al.[61] The cutoff used for molecules subdivision in the two domains during preferential coefficients calculations was chosen considering the distance required for the SDF to approach a unitary value (i.e., bulk distribution), according to previous works.[61]

Protein G B1-(41−56) fragment (GB1-(41−56) peptide) was prepared by automated solid-phase synthesis on an Applied Biosystem Mod 433A synthesizer using 9-fluorenylmethoxycarbonyl (Fmoc) chemistry and Wang resin (Sigma Aldrich). The functional groups of amino acid side chains were protected as follows: Asp(OtBu), Glu(OtBu), Lys-(Boc), Thr(tBu), Tyr(tBu), Trp(Boc). Deprotection and cleavage of the peptide from the resin were performed with TFA/water/1,2-etanedithiol (94:5:1). After purification by semipreparative RP-HPLC (Ascentis C 18, 10 μ, 250 × 10 mm column), the peptide was shown to be >95% homogeneous by analytical RP-HPLC (Ascentis C 18, 5 μ, 250 × 4.6 mm column). Both analytical and preparative runs used gradient elution with A/B mixture from 10 to 30% B in 7 min, to 50% B in 35 min then 100% B in 40 min at 0.5 mL/min (analytical) and 5 mL/min (semipreparative), where A was 0.1% TFA in water and B MeCN/0.1% TFA (8:2). The peptide identity and molecular weight were confirmed by MALDI-TOF mass spectrometry (Bruker Microflex LT Spectrometer), MH^+ at m/z 1864.2, and electrospray ionization mass spectrometry (ESI-MS, ThermoFinnigan LCQ Advantage Spectrometer):, MH+ at m/z 1864.7.

NMR experiments were performed on a Bruker Avance Spectrometer operating at 400.10 1H frequency equipped with a z gradient coil probe. NMR samples were prepared by dissolving GB1-(41−56) peptide in H_2O/D_2O (9:1) or D_2O at a concentration 1 mM. Minute amounts of DCl, NaOD were added to adjust the pH of the samples. Chemical shift values are referenced to TSP (3-(trimethylsilyl) propionic-2,2,3,3-d4 acid sodium salt) as internal standard. All 1D and 2D NMR spectra were collected using the standard pulse sequences available with Bruker Topspin 1.3. Solvent suppression was achieved by including the Excitation Sculpting module in the original 2D TOCSY and NOESY pulse sequences. Short mixing times (200 ms) were used in the NOESY experiments to minimize spin-diffusion effects. Proton resonances were assigned using a combination of DQF-COSY,[62] TOCSY,[63] NOESY.[64] NOE intensities were evaluated by volume integration inspection of the contour levels. Glycine betaine and urea studies were performed through the sequential addition of GB and urea-d4 (Aldrich) to the NMR sample. The conformational shifts (conformation-dependent chemical shifts dispersion) of the Cα protons were obtained by subtracting the random coil values[65] from the measured values for each residue.

■ ASSOCIATED CONTENT

Supporting Information. Additional figures and table. This material is available free of charge via the Internet at http://pubs.acs.org.

■ AUTHOR INFORMATION

Corresponding Author
maurizio.sironi@unimi.it

■ ACKNOWLEDGMENT

We acknowledge the CINECA Award N. HP10BXMGDK, 2010 for the availability of high performance computing resources and support. Aethia is also fully acknowledged for technical assistance.

■ REFERENCES

(1) Yayanos, A. A.; Dietz, A. S.; Boxtel, R. V. *Science* **1979**, *205*, 808.
(2) Nogi, Y.; Kato, C.; Horikoshi, K. *Int. J. Syst. Evol. Microbiol.* **2002**, *52*, 1527.

(3) Yayanos, A. A. *Proc. Natl. Acad. Sci. U.S.A.* **1986**, *83*, 9542.
(4) Takai, K.; Nakamura, K.; Toki, T.; Tsunogai, U.; Miyazaki, M.; Miyazaki, J.; Hirayama, H.; Nakagawa, S.; Nunoura, T.; Horikoshi, K. *Proc. Natl. Acad. Sci. U.S.A.* **2008**, *105*, 10949.
(5) Brochier, C.; Forterre, P.; Gribaldo, S. *Genome Biol.* **2004**, *5*, 17–17.
(6) Furini, A.; Koncz, C.; Salamini, F.; Bartels, D. *EMBO J.* **1997**, *16*, 3599–3608.
(7) Deng, X.; Phillips, J.; Meijer, A. H.; Salamini, F.; Bartels, D. *Plant Mol. Biol.* **2002**, *49*, 601–610.
(8) Yancey, P. H.; Clark, M. E.; Hand, S. C.; Bowlus, R. D.; Somero, G. N. *Science* **1982**, *217*, 1214.
(9) Gillett, M. B.; Suko, J. R.; Santoso, F. O.; Yancey, P. H. *J. Exp. Zool.* **1998**, *279*, 386–391.
(10) Wei, H.; Fan, Y.; Gao, Y. Q. *J. Phys. Chem. B* **2010**, *114*, 557–68.
(11) Beck, D. A. C.; Bennion, B. J.; Alonso, D. O. V.; Daggett, V. *Methods Enzymol.* **2007**, *428*, 373–396.
(12) Bennion, B.; Daggett, V. *Proc. Natl. Acad. Sci. U.S.A.* **2004**, *101*, 6433.
(13) Zou, Q.; Bennion, B.; Daggett, V.; Murphy, K. *J. Am. Chem. Soc.* 2002, *124*, 1192–1202.
(14) Paul, S.; Patey, G. N. *J. Phys. Chem. B* **2008**, *112*, 11106–11.
(15) Xie, G.; Timasheff, S. *Biophys. Chem.* **1997**, *64*, 25–43.
(16) Hu, C. Y.; Kokubo, H.; Lynch, G. C.; Bolen, D. W.; Pettitt, B. M. *Protein Sci.* **2010**, *19*, 1011–1022.
(17) Stumpe, M. C.; Grubmuller, H. *J. Am. Chem. Soc.* **2007**, *129*, 16126–16131.
(18) Hua, L.; Zhou, R.; Thirumalai, D.; Berne, B. J. *Proc. Natl. Acad. Sci. U.S.A.* **2008**, *105*, 16928.
(19) Auton, M.; Holthauzen, L. M.; Bolen, D. W. *Proc. Natl. Acad. Sci. U.S.A.* **2007**, *104*, 15317.
(20) Hu, C. Y.; Pettitt, B. M.; Roesgen, J. *F1000 Biol. Rep.* **2009**, *1*, 41.
(21) O'Brien, E. P.; Ziv, G.; Haran, G.; Brooks, B. R.; Thirumalai, D. *Proc. Natl. Acad. Sci. U.S.A.* **2008**, *105*, 13403–13408.
(22) Rossky, P. J. *Proc. Natl. Acad. Sci. U.S.A.* **2008**, *105*, 16825–6.
(23) Bolen, D. W.; Baskakov, I. V. *J. Mol. Biol.* **2001**, *310*, 955–963.
(24) Bennion, B. J.; Daggett, V. *Proc. Natl. Acad. Sci. U.S.A.* **2003**, *100*, 5142.
(25) Pieraccini, S.; Burgi, L.; Genoni, A.; Benedusi, A.; Sironi, M. *Chem. Phys. Lett.* **2007**, *438*, 298–303.
(26) Civera, M.; Sironi, M.; Fornili, S. L. *Chem. Phys. Lett.* **2005**, *415*, 274–278.
(27) Canchi, D. R.; Paschek, D.; García, A. E. *J. Am. Chem. Soc.* **2010**, *132*, 2338–44.
(28) Gronenborn, A. M.; Filpula, D.; Essig, N.; Achari, A.; Whitlow, M.; Wingfield, P.; GM, C. *Science* **1991**, *253*, 657–661.
(29) Munoz, V.; Thompson, P. A.; Hofrichter, J.; Eaton, W. A. *Nature* **1997**, *390*, 196–198.
(30) Du, D.; Zhu, Y.; Huang, C. Y.; Gai, F. *Proc. Natl. Acad. Sci. U.S.A.* **2004**, *101*, 15915.
(31) Dyer, R. B.; Maness, S. J.; Peterson, E. S.; Franzen, S.; Fesinmeyer, R. M.; Andersen, N. H. *Biochemistry* **2004**, *43*, 11560–11566.
(32) Zagrovic, B.; Sorin, E. J.; Pande, V. *J. Mol. Biol.* **2001**, *313*, 151–169.
(33) Dinner, A. R.; Lazaridis, T.; Karplus, M. *Proc. Natl. Acad. Sci. U. S.A.* **1999**, *96*, 9068.
(34) Shao, Q.; Yang, L.; Gao, Y. Q. *J. Chem. Phys.* **2009**, *130*, 195104.
(35) Nguyen, P. H.; Stock, G.; Mittag, E.; Hu, C. K.; Li, M. S. *Proteins: Struct., Funct,. Bioinf.* **2005**, *61*, 795.
(36) Garcia, A. E.; Sanbonmatsu, K. Y. *Proteins: Struct. Funct. Bioinf.* **2000**, *42*, 345–354.
(37) Bussi, G.; Gervasio, F. L.; Laio, A.; Parrinello, M. *J. Am. Chem. Soc.* **2006**, *128*, 13435.
(38) Bonomi, M.; Branduardi, D.; Gervasio, F. L.; Parrinello, M. *J. Am. Chem. Soc.* **2008**, *130*, 13938–44.
(39) Laio, A.; Parrinello, M. *Proc. Natl. Acad. Sci. U.S.A.* **2002**, *99*, 12562.
(40) Camilloni, C.; Provasi, D.; Tiana, G.; Broglia, R. A. *Proteins: Struct., Funct., Bioinf.* **2008**, *71*, 1647.
(41) Stumpe, M. C.; Grubmüller, H. *Biophys. J.* **2009**, *96*, 3744–52.
(42) Yoda, T.; Sugita, Y.; Okamoto, Y. *Chem. Phys. Lett.* **2004**, *386*, 460–467.
(43) Zhou, R.; Berne, B. J.; Germain, R. *Proc. Natl. Acad. Sci. U.S.A.* **2001**, *98*, 14931.
(44) Blanco, F. J.; Rivas, G.; Serrano, L. *Nat. Struct. Mol. Biol.* **1994**, *1*, 584–590.
(45) Espinosa, J.; Gellman, S. *Angew. Chem., Int. Ed.* **2000**, *39*, 2330–2333.
(46) Bolhuis, P. G. *Proc. Natl. Acad. Sci. U.S.A.* **2003**, *100*, 12129.
(47) Auton, M.; Bolen, D. W. *Proc. Natl. Acad. Sci. U.S.A.* **2005**, *102*, 15065–15068.
(48) Street, T.; Bolen, D.; Rose, G. *Proc. Natl. Acad. Sci. U.S.A.* **2006**, *103*, 13997.
(49) Trzesniak, D.; van Der Vegt, N. F. A.; van Gunsteren, W. F. *Phys. Chem. Chem. Phys.* **2004**, *6*, 697.
(50) Lee, M.-E.; van Der Vegt, N. F. A. *J. Am. Chem. Soc.* **2006**, *128*, 4948–4949.
(51) Lindahl, E.; Hess, B. *J. Mol. Model.* **2001**, 306–317.
(52) Jorgensen, W. L.; Maxwell, D. S.; Tirado-Rives, J. *J. Am. Chem. Soc.* **1996**, *118*, 11225–11236.
(53) Jorgensen, W. L *J. Am. Chem. Soc.* **1981**, *103*, 335–340.
(54) Evans, D. J.; Holian, B. L. *J. Chem. Phys.* **1985**, *83*, 4069.
(55) Darden, T.; York, D.; Pedersen, L. *J. Chem. Phys.* **1993**, *98*, 10089.
(56) Baynes, B. M.; Trout, B. L. *J. Phys. Chem. B* **2003**, *107*, 14058–14067.
(57) Shukla, D.; Shinde, C.; Trout, B. L. *J. Phys. Chem. B* **2009**, *113*, 12546–54.
(58) Vagenende, V.; Yap, M. G. S.; Trout, B. L. *J. Phys. Chem. B* **2009**, *113*, 11743–53.
(59) Kirkwood, J. G.; Goldberg, R. J. *J. Chem. Phys.* **1950**, *18*, 54–57.
(60) Schellman, J. A. *Biopolymers* **1978**, *17*, 1305–1322.
(61) Beck, D. A.; Alonso, D. O.; Daggett, V. *Biophys. Chem.* **2003**, *100*, 221–237.
(62) Derome, A. E.; Williamson, M. P. *J. Magn. Reson.* **1990**, *88*, 177–185.
(63) Griesinger, C.; Otting, G.; Wüthrich, K.; Ernst, R. R. *J. Am. Chem. Soc.* **1988**, *110*, 7870.
(64) Macura, S.; Huang, Y.; Suter, D.; Ernst, R. R. *J. Magn. Reson.* **1981**, *43*, 259–281.
(65) Bundi, A.; Wüthrich, K. *Biopolymers* **1979**, *18*, 285–297.